Chapter 11

NMR Spectroscopy to Study MAP Kinase Binding to MAP Kinase Phosphatases

Wolfgang Peti and Rebecca Page

Abstract

NMR spectroscopy and other solution methods are increasingly being used to obtain novel insights into the mechanisms by which MAPK regulatory proteins bind and direct the activity of MAPKs. Here, we describe how interactions between the MAPK p38α and its regulatory proteins are studied using NMR spectroscopy, isothermal titration calorimetry, and small angle X-ray scattering (SAXS).

Key words Mitogen activated protein kinase (MAPK), p38α, Protein tyrosine phosphatases, Dual specificity phosphatase, Protein–protein interaction, Nuclear magnetic resonance (NMR) spectroscopy, Chemical shift perturbation (CSP), Isotopically labeled growth media, D_2O, Isothermal titration calorimetry (ITC), Small angle X-ray scattering (SAXS)

1 Introduction

Spatial and temporal regulation of mitogen activated protein kinases (MAPKs) is of essential importance for transducing environmental and developmental signals (growth factors, stress) into adaptive and programmed responses (differentiation, inflammation, apoptosis) [1, 2]. Although MAPKs are ubiquitously expressed, their activation is finely tuned in a cell-type specific and temporal manner [3]. The regulators that achieve this fine-tuning include: (1) upstream kinases, (2) downstream phosphatases, and (3) scaffolding proteins [4–6]. Over the years, many groups using a variety of techniques have advanced the field's understanding of how the activities of MAPKs are finely controlled by MAPK regulatory proteins. Clearly, understanding how these proteins interact at a molecular level is also essential [7–15]. X-ray crystallography has provided key insights into the regulation of MAPKs by their interacting proteins by mostly determining structures of MAPKs bound to different peptides derived from interacting proteins [7]; e.g., for the MAPK p38α a single structure of a full-length interacting protein (MK2—a substrate that binds with a K_d of 20 nM) has

Rafael Pulido (ed.), *Protein Tyrosine Phosphatases: Methods and Protocols*, Methods in Molecular Biology, vol. 1447,
DOI 10.1007/978-1-4939-3746-2_11,

Table 1
NMR and SAXS studies of p38α with its regulatory proteins

MAPK complex	Tech	BMRB[b]	Reference
p38α:MKK3b	NMR	6468	[8]
p38α[a]:HePTP$_{15–31}$	NMR	17471/6468	[17]
p38α:HePTP$_{15–56}$	NMR	17471/6468	[17]
p38α:HePTP$_{15–339}$	NMR	17471/6468/15680	[17]
p38α:STEP$_{214–229}$	NMR	17471/6468	[45]
p38α:STEP$_{214–256}$	NMR	17471/6468	[45]
p38α:STEP$_{214–539}$	NMR	17471/19046/6468	[45]
p38α:PTPSL$_{332–348}$	NMR	17471/6468	[45]
p38α:PTPSL$_{332–373}$	NMR	17471/6468	[45]
p38α:PTPSL$_{332–655}$	NMR	17471/6468	[45]
p38α:STEP/PTPSL$_{chimera}$	NMR	17471/6468	[45]
p38α:MKP5/DUSP10	NMR	17471/19330	[58]
*pTpY*p38α[c]:MBP$_{94–102}$	NMR	17940	[59]
p38α:HePTP$_{15–339}$	SAXS	–	[17]
p38α:STEP$_{214–539}$	SAXS	–	[45]
p38α:PTPSL$_{332–655}$	SAXS	–	[45]
p38α:STEP/PTPSL$_{chimera}$	SAXS	–	[45]
p38α:MKP5/DUSP10	SAXS	–	[58]

[a]82% of all expected resonances assigned
[b]BMRB references 6468 [21], 15680 [60], 17471 [17], 17940 [59]
[c]56% of all expected resonances assigned

been determined [16]. Over the last ~10 years, biomolecular NMR spectroscopy has complemented and, more critically, expanded these efforts [17–22]. By doing so, it has become apparent that regulatory proteins adopt distinct conformations when bound to MAPKs and have different degrees of flexibility upon complex formation, which contributes to the observed differences in their biological functions. Here we review the use of biomolecular NMR spectroscopy and other biophysical techniques to study complexes between the MAPK p38α and its regulatory proteins (Table 1).

2 Materials

Prepare all solutions using ultrapure Water (Milli-Q water purification system, Millipore). Chemicals should be at least ACS grade. Prepare and store reagents/solutions at temperatures and

conditions recommended by the manufacturer. Chemicals specific for NMR labeling, e.g., [^{13}C]D-glucose, [^{13}C]D-d^{7}-glucose (1,2,3,4,5,6,6-d^{7}), $^{15}NH_4Cl$, D_2O are typically purchased from Cambridge Isotope Laboratories (CIL) or Isotech (Sigma). Standard buffers are used for purification; when necessary, buffers are autoclaved when prepared in order to prevent unwanted proteolytic degradation. All buffers are stored at 4 °C and are filtered (0.22 μm PES filter, Millipore) prior to use. If possible uniform buffers should be used throughout all experiments. Furthermore, it is important to reduce the salt concentration and select the right buffer for NMR experiments as the sensitivity of cryoprobe significantly decreases with increasing amounts of salt (thus it is also better to use HEPES buffer than phosphate buffer) [23]. Buffers for ITC experiments must be degassed. NMR data analysis can be performed by a variety of software, including Cara (http://cara.nmr.ch), NMRVIEW [24], Sparky [25], and CCPN [26, 27].

1. M9 medium: Weigh 5.8 g Na_2HPO_4 anhydrous, 3.0 g KH_2PO_4, and 0.5 g NaCl. Add water to a volume of 900 mL. Mix and adjust pH to 7.1–7.3 with HCl. Volume up to 1 L with water. Sterilize by filtration and store at 4 °C.
2. Vitamin mix: BME mix (Sigma-Aldrich). Use directly for H_2O-based medium. Lyophilize and resuspend in D_2O for D_2O-based medium.
3. Solution Q: In a final volume of 1 L of water, add 8 mL 5 M HCl (*see* **Note 1**), 5 g $FeCl_2{\cdot}4H_2O$, 184 mg $CaCl_2{\cdot}2H_2O$, 64 mg H_3BO_3, 18 mg $CoCl_2{\cdot}6H_2O$, 4 mg $CuCl_2{\cdot}2H_2O$, 340 mg $ZnCl_2$, and 40 mg $Na_2MoO_4{\cdot}2H_2O$. Mix thoroughly. Aliquot into 2 mL Eppendorf tubes, freeze and store at –20 °C.
4. Glucose: Use [^{12}C]D-glucose for unlabeled protein expression; [^{13}C]D-glucose for ^{13}C labeled protein expression; [^{13}C]D-d^{7}-glucose (1,2,3,4,5,6,6-d^{7}) for fully deuterated protein expression.
5. Ammonium chloride: Use NH_4Cl for unlabeled protein expression and $^{15}NH_4Cl$ for NMR-active protein expression.
6. Preparation of medium: All plastic ware must be autoclaved before use; for large-scale expression we prefer Ultra-Yield 2 L expression flasks (six-times baffled for high aeration; Thomson Instrument Company); 250 mL of media for each Ultra-Yield 2 L expression flask [28].
7. NMR tubes: Different NMR tubes are available for measurements which differ both in diameter (1, 1.7, 3, and 5 mm [outdated: 8 and 10 mm]; 5 mm is the size most commonly used) and shape (distinct shapes can partially compensate the reduced sensitivity of high salt samples in cryo-probes). Shigemi has developed a set of tubes that use solvent-susceptibility matched glass and thus allows for lower sample volumes (~40% reduction), with similar tubes are also available from New Era Scientific.

3 Methods

3.1 Production of p38α and Regulatory Protein Tyrosine Phosphatases for NMR Studies

p38α and its regulatory proteins are large proteins (≥35 kDa) for biomolecular NMR spectroscopy [29, 30]. In order to analyze proteins using NMR spectroscopy, they must be uniformly labeled with NMR-active nuclei. NMR-active nuclei have a nuclear spin, preferably with a spin number of ½ (^{1}H, ^{13}C and ^{15}N nuclei have spin numbers of ½). Labeling is achieved by providing labeled precursors (e.g., [^{13}C]-D-glucose, $^{15}NH_4Cl$) during protein expression in a variety of expression systems, including *Escherichia coli* (*E. coli*) [28], yeast [31], insect cell [32], and human expression systems [33].

However, in order to overcome the broad line-widths that are characteristic of proteins ≥35 kDa, MAPKs must be expressed in D_2O-based medium and TROSY [34] versions of all 2D and 3D experiments must be recorded using a high-field NMR spectrometer (800–1000 MHz ^{1}H Larmor frequency) [35]. Deuteration reduces the dipole–dipole ^{1}H–^{1}H relaxation, as deuterium has a ~7-fold lower gyromagnetic ratio than protons [36]. However, as most NMR experiments rely on the excitation and detection of ^{1}H (largest gyromagnetic ratio; 99.9% natural abundance), deuteration limits the available experimental approaches for such proteins. Most $^{1}H^{N}$ will rapidly back-exchange during protein purification in H_2O-based buffers. However, H/D exchange can be slow in β-sheets and in hydrophobic pockets where access of water or strong hydrogen bonds can significantly limit the exchange rates. If possible, protein refolding either by chemicals or pressure in H_2O-based buffers can be helpful; however, refolding of larger signaling enzymes, such as p38α or tyrosine phosphatases, is not readily achievable. For many years expression of deuterated proteins was limited to the *E. coli* expression system, but recently it has become economically feasible to express ^{2}H-labeled proteins in insect cells [37]. To achieve the necessary high expression yields, *E. coli* cells must be adapted for growth in D_2O-based medium.

3.1.1 Fresh Transformation and Colony Expression Screening

1. Transform the expression plasmid into the appropriate *E. coli* expression cell line (*see* **Notes 2** and **3**).
2. Screen multiple (three to five) colonies for robust expression using a small scale growth and induction (i.e., β-D-1-thiogalactopyranoside [IPTG]) in Luria broth (LB) medium (3–5 mL). Allow expression to proceed for 2 h at 37 °C and evaluate the expression levels of the different colonies using sodium dodecyl sulfate polyacrylamide gel electrophoresis (SDS-PAGE) and Coomassie staining.

3.1.2 D_2O Adaption (see Table 2 and Fig. 1)

1. 20 µL of uninduced LB growth is transferred into 3 mL of freshly prepared 0% D_2O medium and grown for ~12–15 h (37 °C; 250 rpm shaking).

Table 2
D_2O adaption

	0% D_2O (10 mL)	30% D_2O (10 mL)	50% D_2O (10 mL)	70% D_2O (10 mL)	100% D_2O (10 mL)
D_2O	–	3 mL	5 mL	7 mL	8.84 mL
H_2O	8.84 mL	5.84 mL	3.84 mL	1.84 mL	–
10× M9	1 mL	1 mL	1 mL	1 mL	1 mL
1 M $MgSO_4$	20 µL	20 µL	20 µL	20 µL	20 µL
Vitamins	100 µL	100 µL	100 µL	100 µL	100 µL
Solution Q	20 µL	20 µL	20 µL	20 µL	20 µL
Glucose	40 mg	40 mg	40 mg	40 mg	40 mg
NH_4Cl	10 mg	10 mg	10 mg	10 mg	10 mg
Antibiotic	10 µL	10 µL	10 µL	10 µL	10 µL

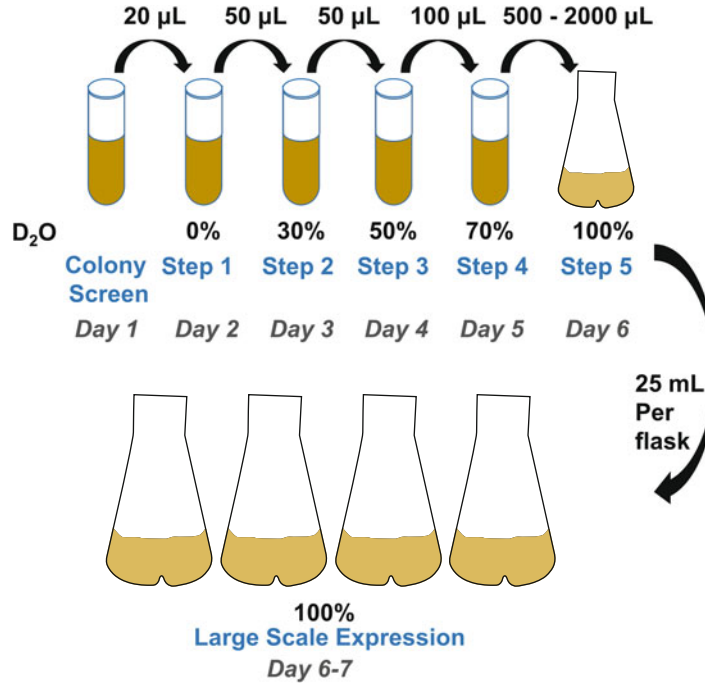

Fig. 1 Schematic of the D_2O adaption protocol. See text for details

2. 50 µL of the 0% D_2O culture is added to 3 mL of 30% D_2O and grown for ~12–15 h (37 °C; 250 rpm shaking).
3. 50 µL of the 30% D_2O culture is added to 3 mL of 50% D_2O and grown for ~12–15 h (37 °C; 250 rpm shaking).

4. 100 µL of the 50% D_2O culture is added to 3 mL of 70% D_2O and grown for ~12–15 h (37 °C; 250 rpm shaking).
5. 500–2000 µL (depending on protein) of the 70% D_2O culture is added to 100 mL of 100% D_2O medium in a 500 mL Ultra-Yield expression flask (*see* **Notes 4** and **5**) and grown for ~12–15 h (37 °C; 250 rpm shaking).

3.1.3 D_2O Large Scale Expression

25 mL of the 100% D_2O culture is added to 225 mL of 100% D_2O medium in a 2 L Ultra-Yield flask and the cells grown to OD_{600} of ~0.6–0.8 (37 °C; 250 rpm shaking with the appropriate antibiotics). Cells are induced using the appropriate induction agent (i.e., IPTG) and then expressed at appropriate temperature (e.g., 18 °C; 18–20 h, 250 rpm shaking for p38α [*see* **Note 6**]). Large scale expression of [^{2}H,^{15}N]-p38α is done in M9 medium supplemented with $^{15}NH_4Cl$ (1 g per 1 L medium) in 99.8% D_2O, and [^{2}H,^{13}C,^{15}N]-p38α is expressed in M9 medium supplemented with $^{15}NH_4Cl$ (1 g per 1 L medium) and [^{13}C]D-d7-glucose (4 g per 1 L medium) in 99.8% D_2O.

3.1.4 D_2O Recycling

D_2O can be readily recycled and reused with a slightly (~10–15%) lower degree of deuteration, which is done in many laboratories.

1. Following the pelleting of the cell mass after the large-scale D_2O expression, the supernatant is collected and stored (RT or –20 °C; *see* **Note 7**).
2. Used D_2O is distilled in a standard glass apparatus, with a controlled heating mantle and a 4 L distillation flask with two inlets (*see* **Note 8**). Aluminum foil is used to lower the boiling temperature. Regular boiling stones are used to ensure to ensure uniform boiling.
3. During distillation, the distillation flask will accumulate debris. Used D_2O is added to the flask until 20–40 L has been distilled. At this point the flask is either cleaned or replaced.
4. Distilled D_2O is perfectly clear; however, it has nasty ammonia-like smell. To make the distilled D_2O suitable for culturing bacteria (*E. coli* will not grow on the freshly distilled, but nasty smelling D_2O), the distilled D_2O must be treated with ~20 g of acid-washed activated charcoal (Sigma) per 1 L of distilled D_2O under vigorous stirring for 12–24 h. The activated carbon is removed by filtering through a Buchner filter.
5. If necessary, the recycled D_2O can be filtered through a 2 µm bottle-top filter to remove any remaining debris/charcoal. At this point, the D_2O is completely clear and does not have any detectable odor. The recycled D_2O can then be used identically to fresh D_2O. Mass spectrometry will confirm a lower rate of deuteration (~85%) (*see* **Note 9**).

3.2 Interaction with Kinase Interaction Motif Protein Tyrosine Phosphatases (KIM-PTPs) and MAPK Protein Tyrosine Phosphatases

Rapid assessment of a protein–protein interaction can be achieved using size exclusion chromatography (SEC) by simply comparing the retention volume (or time) of the free and complex samples. SEC media varies widely in quality and size, leading to different numbers of theoretical plates and thus resolution. For protein studies, Superdex or Sephacryl (GE Healthcare) are the most commonly used media due to their high inertness to nonspecific interactions and their excellent separation capabilities. An earlier eluting peak indicates a higher molecular weight complex and can be readily compared with the SEC of the individual components (proteins). The best readout is SDS-PAGE, where both proteins should be present throughout the peak with similar intensities. In order to measure a full thermodynamic profile of a protein–protein interaction, isothermal titration calorimetry is the best method. Its drawback is the need for rather high amounts of protein. Malvern (VP-ITC and ITC_{200}) and TA Instruments (nano-ITC) are the main manufacturers of these instruments.

1. All ITC experiments should be performed at the same temperature.
2. All proteins and/or peptides must be in the identical buffer (*see* **Note 10**).
3. All proteins should be purified using SEC (e.g., Superdex 75 26/60; GE Healthcare) immediately prior to the experiment.
4. To carry out the ITC experiment, titrant (10 μL per injection) is injected into the sample cell over a period of 20 s with a 250 s interval between titrations to allow for complete equilibration and baseline recovery. About 28 injections are delivered during each experiment (example given for a VP-ITC system), and the solution in the sample cell is stirred at 307 rpm to ensure rapid mixing.
5. Data analysis, Origin: A nonlinear least-squares algorithm and the titrant and sample cell concentrations are used to fit the integrated heat per injection to an equilibrium binding equation, providing values of the stoichiometry (n), change in enthalpy (ΔH) and the binding constant (K). Subsequently, ΔG and ΔS are readily calculated. Data are most commonly analyzed with a one-site binding model assuming a binding stoichiometry of 1:1. Typically, Origin 7.0 software with a specific ITC module is used for data evaluation.
6. Data analysis, NITPIC [38] and SEDPHAT [39]: NITPIC is a stand-alone program that is used to integrate ITC data from a variety of instruments and prepare the data for analysis using SEDPHAT, a program designed to analyze multiple datasets from different biophysical methods, including ITC.

3.3 NMR Spectroscopy

NMR spectroscopy is one of the best techniques to measure interactions (e.g., protein–protein, protein–peptide, protein–DNA, protein–RNA, protein–inhibitor [small molecule], and any variation thereof) at a variety of binding strengths; it is especially well suited to detect weak and even very weak interactions (μM–mM).

3.3.1 NMR Sample Preparation

1. Identification of the optimal sample buffer: Perform a high-throughput buffer screen to identify the buffer, pH, and salt concentration at which the protein is most stable (*see* **Notes 11** and **12**).
2. Identification of the optimal temperature for NMR measurements: The faster a protein tumbles in solution, the shorter its overall correlation time (τ_c) and the better the spectral quality due to longer transverse relation times (R_2). Thus, once the optimal buffer has been identified, determine the melting temperature of the protein and set the measurement temperature at ~30 °C below the melting temperature (*see* **Note 13**).
3. A small amount of D_2O must be added to the sample (1–10% depending on the spectrometer and probe used (*see* **Note 14**).

3.3.2 NMR Experiments, Sequence Specific Backbone Assignment

1. Sequence specific backbone assignment: 2D [^{1}H,^{15}N]-TROSY, 3D HNCA [40], 3D HNCACB, 3D HN(CO)CA, 3D HN(CO)CACB, 3D HNCO, 3D HN(CA)CO, and a 3D ^{15}N-edited [^{1}H,^{1}H] NOESY spectrum are the most common NMR spectra used to achieve the sequence-specific backbone assignment for a protein (*see* **Notes 15** and **16**).
2. Verification of assignment accuracy, single amino acid labeling: Due to the significantly reduced number of experiments (*see* **Note 15**) and the potential reduced completion percentage of the sequence-specific backbone assignment in large proteins due to, for example, the lack of H/D back-exchange, it is critical to verify the accuracy of the assignment. One of the primary methods by which this is achieved is by using single amino acid labeled samples (see examples in [41, 42]), which can be rapidly produced for ^{15}N-Phe, ^{15}N-Ile, ^{15}N-Leu, and ^{15}N-Tyr. Here it is best to use a specially prepared medium that has all amino acids in unlabeled form except for the ones that should be labeled, which are added as ^{15}N-labeled amino acids. As these samples are produced using H_2O and not D_2O, sequence-specific backbone assignment problems arising from D_2O/H_2O back-exchange can be assayed.
3. Verification of assignment accuracy, CSPs: The sequence-specific backbone assignment can be further verified using ligand and/or inhibitor binding. Here, only residues known to interact with the ligand/inhibitor should show significant chemical shift perturbations (CSP) [43]. For example, we used C3′-(2,2,5,5-tetramethyl-3-pyrroline-1-oxyl-3-carboxylic acid

ester) adenosine triphosphate (SL-ATP, a generous gift from Dr. Pia Vogel, Southern Methodist University) [44] to verify the assignment of p38α. AMP-PNP and/or specific p38α inhibitors can be used to test for CSP changes. This allows for the rapid detection of potentially mis-assigned residues.

4. Data deposition: All NMR chemical shift information must be deposited in the BioMagResBank (www.bmrb.wisc.edu; p38α accession number is 17471) so it can be downloaded and used by other research scientists for additional analysis and/or for the design of novel experiments.

3.3.3 NMR Experiments, Protein–Protein Interactions

1. Identification of residues that mediate a protein–protein interaction: The formation of a protein–protein complex influences the local environment of chemical shifts, which can be readily measured using a concentration dependent recording of a series of 2D [^{1}H,^{15}N] HSQC spectra [43]. Specifically, one protein is ^{15}N-labeled (NMR-active) and the second protein is un-labeled (NMR-inactive). The bound, unlabeled protein will change the local environment of the amino acids that mediate binding, which can be readily detected in the NMR spectrum.
2. Measuring the K_d of the interaction: A concentration-dependent measurement is used to determine an amino acid specific K_d. Protein–protein binding events typically lead to a concentration dependent linear change in the chemical shift value. If a deviation from this linear change is detected, this means an additional conformational change is occurring during the binding event (*see* **Note 17**).
3. Reverse titrations: A reverse titration can be performed in which the previous unlabeled protein is now NMR active, while the previous NMR-active protein is now unlabeled. In this way, the complementary binding site can be determined.
4. NMR spectroscopy has a size limit; however, these CSP studies can be performed even with very high molecular weight proteins (depending on the labeling scheme up to 1 MDa). A further advantage of this technique is the ability to use peptides and full length proteins, which allows, for example, a small part of an interaction to be tested via a peptide [17, 45].

3.4 Global Structures

NMR spectroscopy has a limited set of experiments for measuring long-distance interactions. Nuclear Overhauser Effect (nOe) measurements (^{1}H–^{1}H dipole–dipole) are limited to ~5–6 Å (depending on labeling and the size of the B_0 field used for the measurements; NOE scales with $B_0^{3/2}$) [46]. Paramagnetic spin relaxation measurements (^{1}H–e^{-} dipole–dipole) allow for the measurements of longer distances (up to ~20 Å), but require routine modification of the protein (e.g., covalently attached via a cysteine or a

N/C-terminal residue) using a paramagnetic spin label (most commonly used spin-label is (1-Oxyl-2,2,5,5-tetramethylpyrroline-3-methyl)methanethiosulfonate [MTSL]) [47]. As the relaxation effects depend on the internal dynamics of the spin label as well as the proteins themselves, all quantitative distance interpretation of spin-label data must be performed with great care. Other possibilities to define tertiary and quaternary structures are the use of residual dipolar couplings (RDCs) [48]. Rapid isotropic overall tumbling of the proteins in solution usually cancels out dipolar couplings. However, introducing a slight preferred alignment relative to the external field, e.g., through changes in the solution environment or high magnetic field strengths, restores a portion of these couplings. The measurement of these RDC data makes it possible to derive the orientation of a large number of local NH vectors in relationship to the overall alignment tensor, and thus can define the relative orientation of distant parts of for example a multi-domain protein.

Another method to obtain long-distance information is the incorporation of overall distance and shape constrains from independent small angle X-ray scattering measurements (SAXS; this method reports on the isotropic scattering of X-ray photons on proteins in solution, which enables the measurements of the radius of gyration (R_g) among other parameters; *see* ref. 49 for a review). For example, to determine the structure of p38α in complex with HePTP, multiple experiments were performed. X-ray crystallography and NMR spectroscopy were used to achieve a high resolution local structure while SAXS allowed for the description of the global structure [17]. In recent years, a variety of computational methods have been introduced that allow data from multiple techniques to be optimally combined in order to determine the structure and/or the ensemble of structures that best fit the experimental results (HADDOCK [50, 51], EROS [18, 52], EROS-NMR [17], among other software [53]).

SAXS measurements can be performed either at a home source or at a synchrotron. Here we summarize steps we routinely perform when measuring this data.

1. Obtaining non-aggregated samples: SAXS is exceptionally sensitive to aggregation, as soluble aggregates, even if they represent less than 1% of the sample, are significantly larger and thus will have a major impact on the overall measured scattering. Thus, it is optimal to prepare the protein sample immediately (or as shortly as possible before) the SAXS measurements; to facilitate optimal sample preparation, some synchrotron beamlines offer in-line SEC purification prior to SAXS measurements. For some samples, it is possible to filter aggregates prior to measurement. For this, 0.02 μm syringe filters (GE Healthcare Anotop 10) are suitable (*see* **Note 10**).

2. Sample concentration: The optimal concentration for SAXS measurements depends on the X-ray source, the size and assembly of the cell (flow-through or static), among other parameters. For example, on our home source (BioSAXS, FRE+ anode, Rigaku), we measure samples at concentrations as low as 1.5 mg/mL. Typically, we initiate our measurements using samples with the lowest concentration possible. We then concentrate the sample and re-collect the SAXS data from the sample at as high of concentration as can be achieved before aggregation is detected (sometimes this can be as high as 30 mg/mL).
3. Aggregation detection: Some samples are not amenable to SAXS measurements as they exhibit aggregation even at low concentrations. Aggregation is readily detected by observing a concentration dependent change in the R_g as well as a change in the I/c_0 plot. In general, all experimental SAXS curves should be parallel at multiple concentrations; discrepancies are a clear indication of aggregation.
4. Radiation damage: Exposure to high energy photons can induce radiation damage. This is less of an issue at home sources, but can occur when using synchrotron radiation. Here, the use of flow cells can alleviate the problem [54].
5. SAXS data analysis: Numerous software packages are available to analyze SAXS data, with the two most widely used being ATSAS [55] and SCATTER, both of which also allow for the calculation of 3D envelops from the data; this calculations are usually performed with the highest signal/noise dataset (commonly highest measured concentration). This can also be done using Fast-SAXS-pro [56].

4 Notes

1. Warning: HCl must be diluted into H_2O or D_2O; do not add directly to metals.
2. For p38α expression, we use BL21 (DE3) RIL cells (Agilent) to overcome rare codon usage bias in *E. coli*.
3. A fresh transformation is essential for high yield expression of deuterated proteins.
4. 500 mL is the minimum flask volume to ensure sufficient culture aeration.
5. Generally, after the overnight growth step with 70% D_2O-based medium, the 1 L of D_2O-based medium is prepared with 100 mL distributed in a 500 mL Ultra-yield flask and the remaining 900 mL distributed equally into four 2 L Ultra-yield flasks.

6. For proteins that are expressed at 18 °C, cultures must be cooled to 18 °C prior to induction.
7. One typically waits until ~10–20 L of used D_2O have accumulated before initiating D_2O recycling.
8. Flasks with two inlets are optimal because they can be readily refilled.
9. We routinely recycle D_2O twice. The doubly recycled D_2O is only used for test expression, initial protein characterization and protein–protein interaction studies and sequence specific backbone assignment experiments.
10. Typically, we prepare 4–8 L of the appropriate ITC buffer that is then used for all subsequent experiments in order eliminate any heat of dilution from a buffer mismatch. The same approach is used for SAXS measurements, where accurate buffer subtraction is equally important.
11. We use the high-throughput thermofluor assay to identify optimal buffers for NMR samples [57].
12. Modern NMR spectrometers are most commonly equipped with cryogenically cooled NMR probes. Here, cold (~20 K) helium gas is used to cool the coil and the built-in signal preamplifier of the probe, which reduces thermal noise and increases the signal-to-noise ratio by an factor of 3–4. Because cryoprobes are very sensitive to salt concentrations, samples with lower ionic strength ($\leq$50 mM) are preferred. In addition, HEPES should be preferably used over phosphatase buffers.
13. We determine the melting temperature by following the transition of the 222 nM circular dichroism [CD] signal during heating from 25 to 90 °C.
14. The deuterium NMR signal (nuclear spin = 1) is used as an internal reference and allows for rapid compensation for changes of the magnetic field due to environmental changes (cars on nearby roads, etc.) or the stability of the superconductive magnet.
15. Due to their large gyromagnetic ratio, protons (42.58 MHz/T; ratio of magnetic dipole moment/angular momentum of proton) are most commonly used for excitation and detection of NMR experiments. Thus, in fully deuterated samples, where the only H_2O exchangeable protons are available for excitation and detection (specifically $^1H^N$), the number of useable NMR experiments are significantly reduced.
16. The sequence-specific backbone assignment allows for the identification (assignment) of each peak in an NMR spectrum specifically to its amino acid and atom in the protein under investigation. It is based on probability matching of measured chemical shifts—thus, the more the data points, the higher the

likelihood of a correct assignment. As a consequence, the higher the completion percentage of the sequence-specific backbone assignment is, the smaller the chance of errors in the sequence-specific backbone assignment.

17. Depending on the K_d, the interaction will be in the fast, intermediate or slow exchange regime. A fast and slow exchange regime titration can be most readily analyzed. In the fast exchange regime, the switching between chemical states is so rapid that one average chemical shift is reported and thus the change can be fully traced (K_d μM range). Here the experimenter needs to use ratios of 1:1, 1:2, 1:3, and higher until full saturation is achieved, i.e., until the peaks do not shift further upon the addition of more protein. An interaction in the slow exchange regime will lead to two peaks, whose intensities reflect their populations. An interaction in the intermediate exchange regime often leads to a broadening of the peaks beyond detectability. Here titration ratios of 1:0.1, 1:0.25, 1:0.5, etc. can be useful to be able to trace changes.

Acknowledgement

The authors thank the large numbers of highly skilled and ambitious coworkers for their strong support in the effort to better understand protein phosphatases. They are also deeply indebted to many members of the phosphatase field—too many to name—for their support, for their collaborations and their input. We thank Dr. Michael Clarkson (Brown University) for input for the document and Dr. Andrew Hink (UTHSCSA) for input in regard to D_2O recycling. This work was supported by NIH grant R01GM098482 to RP, R01GM100910 to WP.

References

1. Cuadrado A, Nebreda AR (2010) Mechanisms and functions of p38 MAPK signalling. Biochem J 429(3):403–417. doi:10.1042/BJ20100323, BJ20100323 [pii]
2. Kim EK, Choi EJ (2010) Pathological roles of MAPK signaling pathways in human diseases. Biochim Biophys Acta 1802(4):396–405. doi:10.1016/j.bbadis.2009.12.009, S0925-4439(10)00015-3 [pii]
3. Coulthard LR, White DE, Jones DL, McDermott MF, Burchill SA (2009) p38(MAPK): stress responses from molecular mechanisms to therapeutics. Trends Mol Med 15(8):369–379. doi:10.1016/j.molmed.2009.06.005, S1471-4914(09)00114-2 [pii]
4. Brown MD, Sacks DB (2009) Protein scaffolds in MAP kinase signalling. Cell Signal 21(4):462–469. doi:10.1016/j.cellsig.2008.11.013, S0898-6568(08)00345-8 [pii]
5. Imajo M, Tsuchiya Y, Nishida E (2006) Regulatory mechanisms and functions of MAP kinase signaling pathways. IUBMB Life 58(5–6):312–317. doi:10.1080/15216540600746393, N77103R4L425G181 [pii]
6. Koveal D, Schuh-Nuhfer N, Ritt D, Page R, Morrison DK, Peti W (2012) A CC-SAM, for coiled coil-sterile alpha motif, domain targets the scaffold KSR-1 to specific sites in the plasma membrane. Sci Signal 5(255):ra94. doi:10.1126/scisignal.2003289

7. Peti W, Page R (2013) Molecular basis of MAP kinase regulation. Protein Sci 22(12):1698–1710. doi:10.1002/pro.2374
8. Akella R, Min X, Wu Q, Gardner KH, Goldsmith EJ (2010) The third conformation of p38alpha MAP kinase observed in phosphorylated p38alpha and in solution. Structure 18(12):1571–1578. doi:10.1016/j.str.2010.09.015, S0969-2126(10)00368-0 [pii]
9. Akella R, Moon TM, Goldsmith EJ (2008) Unique MAP kinase binding sites. Biochim Biophys Acta 1784(1):48–55. doi:10.1016/j.bbapap.2007.09.016,S1570-9639(07)00281-6 [pii]
10. Canagarajah BJ, Khokhlatchev A, Cobb MH, Goldsmith EJ (1997) Activation mechanism of the MAP kinase ERK2 by dual phosphorylation. Cell 90(5):859–869, S0092-8674(00)80351-7 [pii]
11. Chang CI, Xu BE, Akella R, Cobb MH, Goldsmith EJ (2002) Crystal structures of MAP kinase p38 complexed to the docking sites on its nuclear substrate MEF2A and activator MKK3b. Mol Cell 9(6):1241–1249, S1097276502005257 [pii]
12. Goldsmith EJ, Akella R, Min X, Zhou T, Humphreys JM (2007) Substrate and docking interactions in serine/threonine protein kinases. Chem Rev 107(11):5065–5081. doi:10.1021/cr068221w
13. Wang Z, Harkins PC, Ulevitch RJ, Han J, Cobb MH, Goldsmith EJ (1997) The structure of mitogen-activated protein kinase p38 at 2.1-A resolution. Proc Natl Acad Sci U S A 94(6):2327–2332
14. Wilson KP, Fitzgibbon MJ, Caron PR, Griffith JP, Chen W, McCaffrey PG, Chambers SP, Su MS (1996) Crystal structure of p38 mitogen-activated protein kinase. J Biol Chem 271(44):27696–27700
15. Zhou T, Sun L, Humphreys J, Goldsmith EJ (2006) Docking interactions induce exposure of activation loop in the MAP kinase ERK2. Structure 14(6):1011–1019. doi:10.1016/j.str.2006.04.006, S0969-2126(06)00222-X [pii]
16. ter Haar E, Prabhakar P, Prabakhar P, Liu X, Lepre C (2007) Crystal structure of the p38 alpha-MAPKAP kinase 2 heterodimer. J Biol Chem 282(13):9733–9739. doi:10.1074/jbc.M611165200, M611165200 [pii]
17. Francis DM, Rozycki B, Koveal D, Hummer G, Page R, Peti W (2011) Structural basis of p38alpha regulation by hematopoietic tyrosine phosphatase. Nat Chem Biol 7(12):916–924. doi:10.1038/nchembio.707
18. Francis DM, Rozycki B, Tortajada A, Hummer G, Peti W, Page R (2011) Resting and active states of the ERK2:HePTP complex. J Am Chem Soc 133(43):17138–17141. doi:10.1021/ja2075136
19. Piserchio A, Francis DM, Koveal D, Dalby KN, Page R, Peti W, Ghose R (2012) Docking interactions of hematopoietic tyrosine phosphatase with MAP kinases ERK2 and p38alpha. Biochemistry 51(41):8047–8049. doi:10.1021/bi3012725
20. Piserchio A, Warthaka M, Devkota AK, Kaoud TS, Lee S, Abramczyk O, Ren P, Dalby KN, Ghose R (2011) Solution NMR insights into docking interactions involving inactive ERK2. Biochemistry 50(18):3660–3672. doi:10.1021/bi2000559
21. Vogtherr M, Saxena K, Grimme S, Betz M, Schieborr U, Pescatore B, Langer T, Schwalbe H (2005) NMR backbone assignment of the mitogen-activated protein (MAP) kinase p38. J Biomol NMR 32(2):175. doi:10.1007/s10858-005-2449-x
22. Vogtherr M, Saxena K, Hoelder S, Grimme S, Betz M, Schieborr U, Pescatore B, Robin M, Delarbre L, Langer T, Wendt KU, Schwalbe H (2006) NMR characterization of kinase p38 dynamics in free and ligand-bound forms. Angew Chem Int Ed Engl 45(6):993–997. doi:10.1002/anie.200502770
23. Wong M, Khirich G, Loria JP (2013) What's in your buffer? Solute altered millisecond motions detected by solution NMR. Biochemistry 52(37):6548–6558. doi:10.1021/bi400973e
24. Johnson BA (2004) Using NMRView to visualize and analyze the NMR spectra of macromolecules. Methods Mol Biol 278:313–352. doi:10.1385/1-59259-809-9:313
25. Lee W, Tonelli M, Markley JL (2015) NMRFAM-SPARKY: enhanced software for biomolecular NMR spectroscopy. Bioinformatics 31(8):1325–1327. doi:10.1093/bioinformatics/btu830
26. Vranken WF, Boucher W, Stevens TJ, Fogh RH, Pajon A, Llinas M, Ulrich EL, Markley JL, Ionides J, Laue ED (2005) The CCPN data model for NMR spectroscopy: development of a software pipeline. Proteins 59(4):687–696. doi:10.1002/prot.20449
27. Skinner SP, Goult BT, Fogh RH, Boucher W, Stevens TJ, Laue ED, Vuister GW (2015) Structure calculation, refinement and validation using CcpNmr Analysis. Acta Crystallogr D Biol Crystallogr 71(Pt 1):154–161. doi:10.1107/S1399004714026662
28. Peti W, Page R (2007) Strategies to maximize heterologous protein expression in Escherichia coli with minimal cost. Protein Expr Purif 51(1):1–10. doi:10.1016/j.pep.2006.06.024, S1046-5928(06)00195-1 [pii]

29. Tugarinov V, Hwang PM, Kay LE (2004) Nuclear magnetic resonance spectroscopy of high-molecular-weight proteins. Annu Rev Biochem 73:107–146. doi:10.1146/annurev.biochem.73.011303.074004
30. Frueh DP (2014) Practical aspects of NMR signal assignment in larger and challenging proteins. Prog Nucl Magn Reson Spectrosc 78:47–75. doi:10.1016/j.pnmrs.2013.12.001
31. Sugiki T, Ichikawa O, Miyazawa-Onami M, Shimada I, Takahashi H (2012) Isotopic labeling of heterologous proteins in the yeast Pichia pastoris and Kluyveromyces lactis. Methods Mol Biol 831:19–36. doi:10.1007/978-1-61779-480-3_2
32. Gossert AD, Jahnke W (2012) Isotope labeling in insect cells. Adv Exp Med Biol 992:179–196. doi:10.1007/978-94-007-4954-2_10
33. Hansen AP, Petros AM, Mazar AP, Pederson TM, Rueter A, Fesik SW (1992) A practical method for uniform isotopic labeling of recombinant proteins in mammalian cells. Biochemistry 31(51):12713–12718
34. Pervushin K, Riek R, Wider G, Wüthrich K (1997) Attenuated T2 relaxation by mutual cancellation of dipole-dipole coupling and chemical shift anisotropy indicates an avenue to NMR structures of very large biological macromolecules in solution. Proc Natl Acad Sci U S A 94(23):12366–12371
35. Barrett PJ, Chen J, Cho MK, Kim JH, Lu Z, Mathew S, Peng D, Song Y, Van Horn WD, Zhuang T, Sonnichsen FD, Sanders CR (2013) The quiet renaissance of protein nuclear magnetic resonance. Biochemistry 52(8):1303–1320. doi:10.1021/bi4000436
36. Gardner KH, Kay LE (1998) The use of 2H, 13C, 15N multidimensional NMR to study the structure and dynamics of proteins. Annu Rev Biophys Biomol Struct 27:357–406. doi:10.1146/annurev.biophys.27.1.357
37. Sitarska A, Skora L, Klopp J, Roest S, Fernandez C, Shrestha B, Gossert AD (2015) Affordable uniform isotope labeling with H, C and N in insect cells. J Biomol NMR. doi:10.1007/s10858-015-9935-6
38. Keller S, Vargas C, Zhao H, Piszczek G, Brautigam CA, Schuck P (2012) High-precision isothermal titration calorimetry with automated peak-shape analysis. Anal Chem 84(11):5066–5073. doi:10.1021/ac3007522
39. Zhao H, Piszczek G, Schuck P (2015) SEDPHAT—a platform for global ITC analysis and global multi-method analysis of molecular interactions. Methods 76:137–148. doi:10.1016/j.ymeth.2014.11.012
40. Bax A, Ikura M (1991) An efficient 3D NMR technique for correlating the proton and 15N backbone amide resonances with the alpha-carbon of the preceding residue in uniformly 15N/13C enriched proteins. J Biomol NMR 1(1):99–104
41. Francis DM, Page R, Peti W (2014) Sequence-specific backbone (1)H, (1)(3)C and (1)(5)N assignments of the 34 kDa catalytic domain of PTPN5 (STEP). Biomol NMR Assign 8(1):185–188. doi:10.1007/s12104-013-9480-8
42. Krishnan N, Koveal D, Miller DH, Xue B, Akshinthala SD, Kragelj J, Jensen MR, Gauss CM, Page R, Blackledge M, Muthuswamy SK, Peti W, Tonks NK (2014) Targeting the disordered C terminus of PTP1B with an allosteric inhibitor. Nat Chem Biol 10(7):558–566. doi:10.1038/nchembio.1528
43. Williamson MP (2013) Using chemical shift perturbation to characterise ligand binding. Prog Nucl Magn Reson Spectrosc 73:1–16. doi:10.1016/j.pnmrs.2013.02.001
44. Hoffman AD, Urbatsch IL, Vogel PD (2010) Nucleotide binding to the human multidrug resistance protein 3, MRP3. Protein J 29(5):373–379. doi:10.1007/s10930-010-9262-4
45. Francis DM, Kumar GS, Koveal D, Tortajada A, Page R, Peti W (2013) The differential regulation of p38alpha by the neuronal kinase interaction motif protein tyrosine phosphatases, a detailed molecular study. Structure 21(9):1612–1623. doi:10.1016/j.str.2013.07.003
46. Wüthrich K (1986) NMR of proteins and nucleic acids. Wiley-Interscience, New York
47. Gaponenko V, Howarth JW, Columbus L, Gasmi-Seabrook G, Yuan J, Hubbell WL, Rosevear PR (2000) Protein global fold determination using site-directed spin and isotope labeling. Protein Sci 9(2):302–309. doi:10.1110/ps.9.2.302
48. Tolman JR, Flanagan JM, Kennedy MA, Prestegard JH (1995) Nuclear magnetic dipole interactions in field-oriented proteins: information for structure determination in solution. Proc Natl Acad Sci U S A 92(20):9279–9283
49. Rambo RP, Tainer JA (2013) Super-resolution in solution X-ray scattering and its applications to structural systems biology. Annu Rev Biophys 42:415–441. doi:10.1146/annurev-biophys-083012-130301
50. de Vries SJ, van Dijk AD, Krzeminski M, van Dijk M, Thureau A, Hsu V, Wassenaar T, Bonvin AM (2007) HADDOCK versus HADDOCK: new features and performance of HADDOCK2.0 on the CAPRI targets. Proteins 69(4):726–733. doi:10.1002/prot.21723
51. Dominguez C, Boelens R, Bonvin AM (2003) HADDOCK: a protein-protein docking

approach based on biochemical or biophysical information. J Am Chem Soc 125(7):1731–1737. doi:10.1021/ja026939x

52. Rozycki B, Kim YC, Hummer G (2011) SAXS ensemble refinement of ESCRT-III CHMP3 conformational transitions. Structure 19(1): 109–116.doi:10.1016/j.str.2010.10.006,S0969-2126(10)00395-3 [pii]
53. Yang S, Blachowicz L, Makowski L, Roux B (2010) Multidomain assembled states of Hck tyrosine kinase in solution. Proc Natl Acad Sci U S A 107(36):15757–15762. doi:10.1073/pnas.1004569107, 1004569107 [pii]
54. Allaire M, Yang L (2011) Biomolecular solution X-ray scattering at the National Synchrotron Light Source. J Synchrotron Radiat 18(1):41–44. doi:10.1107/S0909049510036022
55. Petoukhov MV, Franke D, Shkumatov AV, Tria G, Kikhney AG, Gajda M, Gorba C, Mertens HD, Konarev PV, Svergun DI (2012) New developments in the program package for small-angle scattering data analysis. J Appl Crystallogr 45(Pt 2):342–350. doi:10.1107/S0021889812007662
56. Ravikumar KM, Huang W, Yang S (2013) Fast-SAXS-pro: a unified approach to computing SAXS profiles of DNA, RNA, protein, and their complexes. J Chem Phys 138(2):024112. doi:10.1063/1.4774148
57. Romanuka J, van den Bulke H, Kaptein R, Boelens R, Folkers GE (2009) Novel strategies to overcome expression problems encountered with toxic proteins: application to the production of Lac repressor proteins for NMR studies. Protein Expr Purif 67(2):104–112. doi:10.1016/j.pep.2009.05.008
58. Kumar GS, Zettl H, Page R, Peti W (2013) Structural basis for the regulation of the mitogen-activated protein (MAP) kinase p38alpha by the dual specificity phosphatase 16 MAP kinase binding domain in solution. J Biol Chem 288(39):28347–28356. doi:10.1074/jbc.M113.499178
59. Nielsen G, Schwalbe H (2011) NMR spectroscopic investigations of the activated p38alpha mitogen-activated protein kinase. Chembiochem 12(17):2599–2607. doi:10.1002/cbic.201100527
60. Jeeves M, McClelland DM, Barr AJ, Overduin M (2008) Sequence-specific 1H, 13C and 15N backbone resonance assignments of the 34 kDa catalytic domain of human PTPN7. Biomol NMR Assign 2(2):101–103. doi:10.1007/s12104-008-9095-7